

AD-A126 188

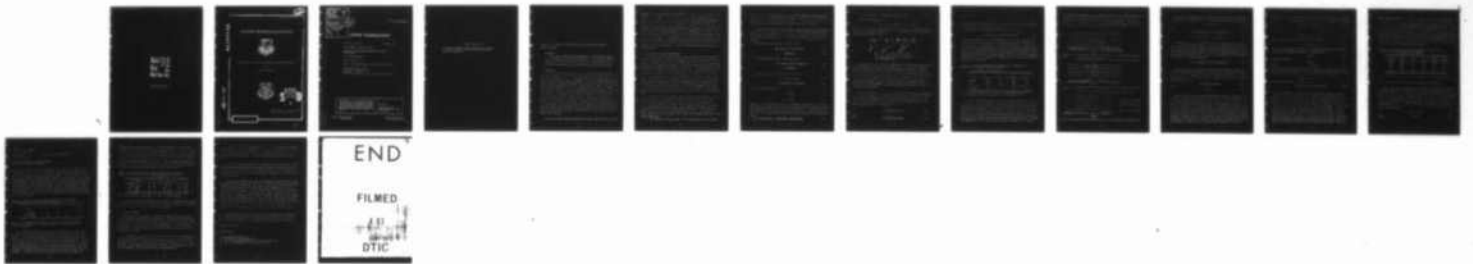
SELECTION OF REPETITION FREQUENCIES FOR LASER  
RANGEFINDERS(U) FOREIGN TECHNOLOGY DIV WRIGHT-PATTERSON  
AFB OH C ZHANG 27 JAN 83 FTD-ID(RS)T-1342-82

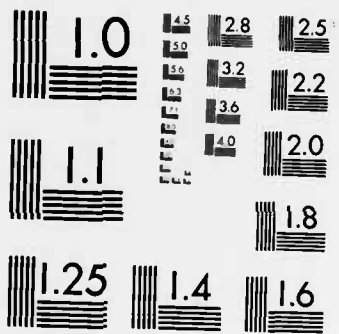
1/1

UNCLASSIFIED

F/G 20/5

NL





MICROCOPY RESOLUTION TEST CHART  
NATIONAL BUREAU OF STANDARDS-1963-A

2

FTD-ID(RS)T-1342-82

ADA 126188

# FOREIGN TECHNOLOGY DIVISION



SELECTION OF REPETITION FREQUENCIES FOR LASER RANGEFINDERS

by

Zhang Chengquan



**S** DTIC  
ELECTE **D**  
MAR 30 1983  
**D**

DTIC FILE COPY

Approved for public release;  
distribution unlimited.



83 03 29 095

Accession For	
NTIS GRA&I	<input checked="" type="checkbox"/>
DTIC TAB	<input type="checkbox"/>
Unannounced	<input type="checkbox"/>
Justification	
By _____	
Distribution/	
Availability Codes	
Dist	Avail and/or Special
A	



FTD-ID(RS)T-1342-82

**EDITED TRANSLATION**

FTD-ID(RS)T-1342-82

27 January 1983

MICROFICHE NR: FTD-83-C-000090

SELECTION OF REPETITION FREQUENCIES FOR LASER  
RANGEFINDERS

By: Zhang Chengquan

English pages: 12

Source: Binggong Xuebao, Nr. 2, May 1982, pp. 34-41

Country of origin: China

Translated by: Randy Dorsey

Requester: FTD/TQCS

Approved for public release; distribution unlimited.

THIS TRANSLATION IS A RENDITION OF THE ORIGINAL FOREIGN TEXT WITHOUT ANY ANALYTICAL OR EDITORIAL COMMENT. STATEMENTS OR THEORIES ADVOCATED OR IMPLIED ARE THOSE OF THE SOURCE AND DO NOT NECESSARILY REFLECT THE POSITION OR OPINION OF THE FOREIGN TECHNOLOGY DIVISION.

PREPARED BY:

TRANSLATION DIVISION  
FOREIGN TECHNOLOGY DIVISION  
WP-AFB, OHIO.

FTD -ID(RS)T-1342-82

Date 27 Jan 19 83

GRAPHICS DISCLAIMER

All figures, graphics, tables, equations, etc. merged into this translation were extracted from the best quality copy available.

## SELECTION OF REPETITION FREQUENCIES FOR LASER RANGEFINDERS

Zhang Chengquan

### ABSTRACT

This paper presents some methods for determining repetition frequencies for laser rangefinders. Using these methods, repetition frequencies for air-to-air, air-to-ground, and ground-to-air laser rangefinders can be correctly selected.

### I. FOREWORD

Laser rangefinders are noted for high rangefinding accuracy, low bulk, light weight, good antig jamming ability, and excellent low-altitude performance, and at present they have obtained wide use in various types of fire control systems. Since the high speed of the target, the interceptor aircraft, or both gives rise to a rapid relative motion between the weapon system and the target, in laser rangefinders used for small antiaircraft guns and aircraft fire control systems, lowering the repetition frequency will not ensure the hit accuracy of the weapon system; raising it is also not necessary and, likewise, it does not help to increase the bulk, the weight, or the power consumption. Therefore, how to rationally select rangefinder repetition frequencies (hereafter called simply repetition frequencies) becomes a crucial problem which must be solved when designing ground-to-air, air-to-ground, and air-to-air type laser rangefinders.

The fire control system requires real-time input into it of the

target distance in order to calculate the moment to fire or the lead angle of the weapon. For a moving target, the process of measuring target distance is essentially the process of carrying out sampling of continuously changing distance values. Based on the sampling theorem [1], when the sampling frequency is equal to or more than two times the maximum frequency  $f_m$  contained in the signal (assuming the frequency has a finite bandwidth, i.e.,  $-f_m < f < f_m$ ), it will be able to pass through an ideal low-pass filter and the original signal will be extracted intact. Consequently, the selection of rangefinder repetition frequencies is summed up as the problem of conducting spectral analysis on target distance information in order to determine its maximum frequency component. Below we discuss two types of laser rangefinders.

## II. AIR-TO-AIR LASER RANGEFINDERS

We used a typical aircraft fire control system as an example to conduct analysis on repetition frequencies of the air-to-air rangefinder. Aircraft fire control systems often take the plane which is defined by the velocity vectors of both the interceptor aircraft and the target aircraft as the basis of analysis. It is assumed that the target is in uniform linear motion (i.e.,  $\vec{V}_m = \text{const}$ ) and that the interceptor aircraft is in constant speed flight (i.e.,  $V_1 = \text{const}$ ). Since the duration of an air combat attack is normally relatively brief, the range of the projectile relatively short, and the gravitational fall negligible, when the maneuverability of the target is relatively poor (such as a bomber) the above assumed and simplified spatial model is an approximation which holds true [2]. Under these simplified assumptions the following attack courses can be developed [2]:

1. The Pure-Pursuit Attack: The velocity vector of the interceptor aircraft is aimed at the target at all times. Infrared missiles are commonly aimed and launched using this attack mode.

2. The Lead-Pursuit Attack: The velocity vectors of the interceptor aircraft are at all times kept pointed at an impact point where the projectile and the target will collide. At present, a large number of aircraft cannon and rockets are aimed and fired using this attack mode.

3. The Lead-Collision Attack: The interceptor aircraft flies

at a constant heading aimed at a projectile-target collision point which is at a preselected launch range. This attack mode normally is used for launching high-powered missiles or rocket salvos and requires much less maneuverability of the interceptor aircraft.

The characteristics of these three attack courses can be shown by fire control triangles as in Figure 1. In the target polar coordinate system, approach angle  $q$  and relative distance  $D$  are taken as the main parameters and the following fire control equations can be obtained

for pure-pursuit attack, see Fig. 1(a);

$$\dot{D} = -V_m \cos q - V_1 = -V_m (\cos q + K) \quad (1)$$

$$\dot{q}D = V_m \sin q \quad (2)$$

for lead-pursuit attack, see Fig. 1(b);

$$\dot{D} = -V_m \cos q - V_1 \cos \varphi \approx -V_m (\cos q + K) \quad (3)$$

$$\dot{q}D = \alpha V_m \sin q \quad (4)$$

and lead-collision attack, see Fig. 1(c).

$$\dot{D} = -V_m (\cos q + K \cos \varphi) \quad (5)$$

$$D = V_m T \cos q + (V_1 T + D_{x_0}) \cos \varphi \quad (6)$$

In the above expressions,

$$K = \frac{V_1}{V_m} \quad (7)$$

$$\alpha = 1 - \frac{V_1}{V_{dp}} \quad (8)$$

where  $V_1$  is the velocity of the interceptor aircraft,  $V_m$  is the velocity of the target,  $V_{dp}$  is the mean velocity of the projectile,  $\varphi$  is the lead angle,  $D_{x_0}$  is the preset relative range. From expressions (1) ~ (6) it is not difficult to derive the relative trajectory equations

$$\text{for pure-pursuit, } D \operatorname{tg}^2(q/2) \sin q = D_0 \operatorname{tg}^2(q_0/2) \sin q_0 \quad (9)$$



for lead-pursuit,  $D^* \text{tg}^2(q/2) \sin q = D_0^* \text{tg}^2(q_0/2) \sin q_0$  (10)

and for lead-collision

$$D = \frac{D_0 \sin \lambda}{\sin q [1 + (V_1/V_m) \cos \lambda] - (V_1/V_m) \sin \lambda \cos q} \quad (11)$$

where  $\lambda$  is the course intersection angle;  $D_0$  and  $q_0$  are the relative distance and approach angle when  $t = 0$ , also called initial distance and occupied approach angle.

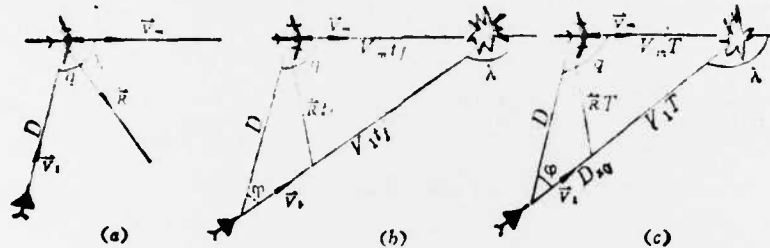


Fig. 1. Fire Control Triangles

- (a) pure-pursuit; (b) lead-pursuit;
- (c) lead-collision

The problem now is to derive equations of distance with change in time, beginning with the above equations, then carry out Fourier transformation and find the maximum frequency component. However, for pure-pursuit and lead-pursuit there are no analytical solutions for distance with change in time. For the former we conducted numerical solutions based on the Parseval theorem [3] with the aid of an electronic computer; for the latter we used Guillemin's impulse approximation method [2, 4] to conduct frequency spectrum analysis. We introduce these below.

From expressions (2), (4), (9), and (10), taking  $q$  as a parameter to carry out numerical integration we can obtain a numerical solution for distance information  $D(t)$  for both the pure-pursuit and lead-pursuit attack courses. Thus, based on the Parseval theorem, the total energy value of the signal is

$$W = \int_{-\infty}^{+\infty} D(t) D^*(t) dt \quad (12)$$

and

$$W = \int_{-\infty}^{+\infty} S(f) S^*(f) df \quad (13)$$

where

$$S(f) = \int_{-\infty}^{+\infty} D(t) e^{-j2\pi ft} dt \quad (14)$$

is the Fourier transform for  $D(t)$ ;  $S(f)S^*(f) = |S(f)|^2$  is called the energy spectrum density function of  $D(t)$ . Thus we can find the energy contained within any given bandwidth  $(-f, +f)$  as

$$W_f = \int_{-f}^{+f} |S(f)|^2 df = \int_{-f}^{+f} S(f)S^*(f) df \quad (15)$$

Comparing expression (15) to expression (12), we can then use the frequency components obtained when  $W_f/W$  arbitrarily approaches 1 (such as 0.99) as the maximum frequency component  $f_m$ . Based on the above, we used a DJS-14 computer to find the energy spectrum densities for  $D(t)$  under conditions of pure-pursuit and lead-pursuit as shown in Figures 2 and 3, respectively. Table 1 shows the frequency component  $f_m$  which corresponds to  $W_f/W=0.99$  as well as the required repetition frequency  $f$ .

Table 1. The Minimum Repetition Frequency  $f$  required for rangefinding during air-to-air attacks

( $V_m=500\text{m/s}$ ,  $K=1.2$ ,  $\alpha=0.5$ )

攻击方式	$D_0$ (b) (米)	$q_0$ (c) (度)	$f_m$ (d) (赫)	$f=2f_m$ (e) (次/秒)
纯追踪 (f)	5,000	90°	1.53	3.06
	5,000	150°	0.38	0.76
	10,000	90°	0.56	1.12
	10,000	150°	0.19	0.38
前置追踪 (g)	2,000	90°	4.00	8.00
	2,000	150°	1.11	2.22

KEY: (a) attack mode; (b) meters; (c) degrees; (d) Hertz; (e) times/second; (f) pure-pursuit; (g) lead-pursuit

It can be seen from Table 1 that when target velocity  $V_m$ , velocity ratio  $K$ , and coefficient  $\alpha$  are fixed, the required repetition frequency  $f$  increases as the initial distance  $D_0$  and occupied approach angle  $q_0$  decrease. These results coincide with the characteristics of the energy spectrum curves in Figures 2 and 3. From Figures 2 and 3 we can see that when the numerical values of  $D_0$  and  $q_0$  are relatively large, the energy spectrum curves are rather pointed, the amplitude of the peak values is high, and there is an ample

low-frequency component; as  $D_0$  and  $q_0$  decrease, the energy spectrum curves gradually level out, the amplitude of the peak value drops, and the high-frequency component noticeably increases. This is because, for a given course of attack, as  $D_0$  and  $q_0$  decrease, the relative distances change more rapidly with change in time.

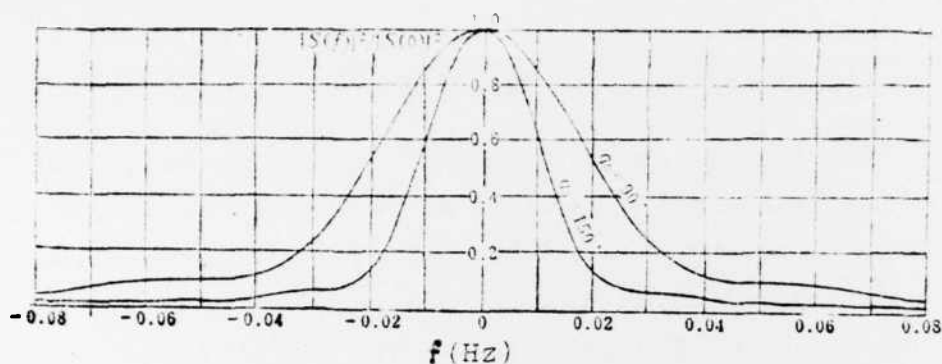


Fig. 2(a). Energy spectrum density for  $D(t)$  in pure-pursuit attack mode

$D_0 = 5000\text{m}, V_m = 500\text{m/s}, K = 1.2;$   
 $|S(0)|^2 = 1.98 \times 10^9, \text{ when } q_0 = 90^\circ, \quad |S(0)|^2 = 1.24 \times 10^{10} \text{ when } q_0 = 150^\circ$

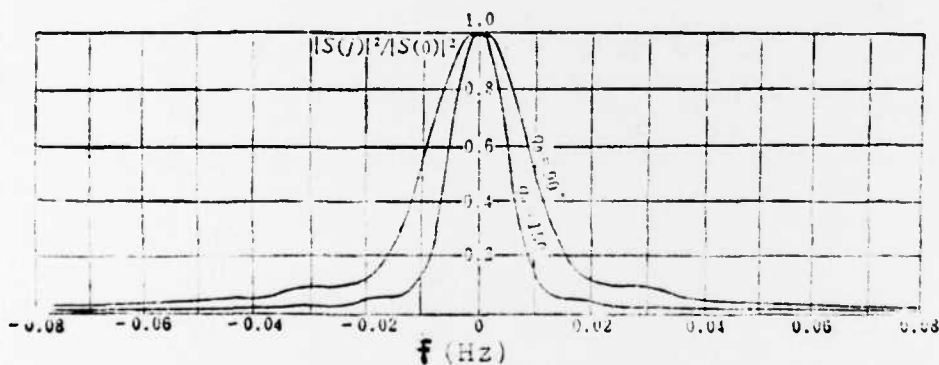
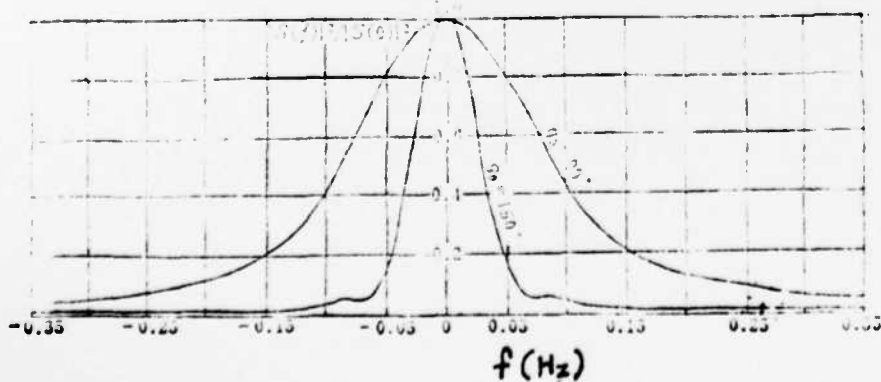


Fig. 2(b). Energy spectrum density for  $D(t)$  in pure-pursuit attack mode

$D_0 = 10,000\text{m}, V_m = 500\text{m/s}, K = 1.2;$   
 $|S(0)|^2 = 3.12 \times 10^{12}, \text{ when } q_0 = 90^\circ, \quad |S(0)|^2 = 1.93 \times 10^{14} \text{ when } q_0 = 150^\circ$



$D_0 = 2000\text{m}, V_m = 500\text{m/s},$   
 $K = 1.2, a = 0.5;$   
 $|S(0)|^2 = 2.14 \times 10^7, \text{ when } q_0 = 90^\circ,$   
 $|S(0)|^2 = 2.72 \times 10^8 \text{ when } q_0 = 150^\circ$

Fig. 3. Energy spectrum density for  $D(t)$  in lead-pursuit attack mode

For the lead-pursuit attack mode the relative motion trajectory is described by expression (11). Expression (11) can be rewritten as

$$D = P / \cos(\varphi - \alpha) \quad (16)$$

where

$$P = D_{r_0} \sin \lambda / \left\{ \left( \frac{V_1}{V_m} \sin \lambda \right)^2 + \left( 1 + \frac{V_1}{V_m} \cos \lambda \right)^2 \right\}^{1/2} \quad (17)$$

$$\alpha = \text{tg}^{-1} \left\{ - \left( 1 + \frac{V_1}{V_m} \cos \lambda \right) / \left( \frac{V_1}{V_m} \sin \lambda \right) \right\} \quad (18)$$

Expression (16) is the standard form for "equations of a line" in the polar coordinate system, while P is the distance between the line in question and the origin of the coordinates, which we call pass-course slant range, and  $\alpha$  is its polar coordinate angle. From fire control triangle Figure 1(c) it is not difficult to find that the velocity of relative motion is

$$\dot{R} \equiv V = V_m \left\{ \left( \frac{V_1}{V_m} \sin \lambda \right)^2 + \left( 1 + \frac{V_1}{V_m} \cos \lambda \right)^2 \right\}^{1/2} \quad (19)$$

Since the course intersection angle  $\lambda$  is constant in the lead-collision attack, the value of V is constant. This shows that the relative motion is uniform velocity, straight-line motion. Assuming pass-course time of  $t=0$ , we obtain an equation for relative distance with change in time

$$D(t) = P \{ 1 + (t/\tau)^2 \}^{1/2} \quad (20)$$

where

$$\tau = P/V \quad (21)$$

Such a time function cannot analytically directly determine the Fourier transform for expression (20). Even if the above method of treatment could be used here to carry out a numerical solution, since we must perform three numerical integrations to determine each point on the  $Wf$  curve and the machine time used will be quite long, we would rather use the Guillemin impulse method to approximate its Laplace transform, then letting  $s = j\omega$  we can determine the frequency spectrum characteristics. The dominant idea of the Guillemin impulse method is converting the integrand in Laplace integration into a set of impulses in order to use the analytical method to carry out

integration. Now letting the Laplace transform approximation expression for  $D(t)$  in expression (20) be  $D^*(S)$ , then from [2,4] we obtain

$$D^*(S)/P = \frac{1}{S^2} - \frac{1}{S^2} (e^{s\tau} - e^{-s\tau}) \quad (22)$$

and letting  $S \rightarrow j\omega$ , we obtain a frequency characteristic of

$$D^*(j\omega)/P = \frac{1}{(j\omega)^2} - \frac{1}{(j\omega)^2} (e^{j\omega\tau} - e^{-j\omega\tau}) \quad (23)$$

Hence, the frequency spectrum function becomes

$$|D^*(j\omega)/P| = 2 \sin \omega\tau / \omega^2 \tau^2 \quad (24)$$

We take the first zero point of the frequency spectrum function as the maximum frequency component. Assuming that

$$\omega_m \tau = \pi \quad (25)$$

and assuming that

$$2\pi f_m \tau = \pi$$

hence

$$f_m = 1/2\tau \quad (26)$$

The problem now is how to find  $\tau$ . Therefore, we must first find course intersection angle  $\lambda$ . Using Figure 1(c), from the theorem of sines we know that  $\lambda$  must satisfy the following expression

$$D_0 / \sin(\pi - \lambda) = (V_1 T + D_{x_0}) / \sin q_0 \quad (27)$$

and from the theorem of cosines we obtain

$$(V_1 T + D_{x_0})^2 = D_0^2 + (V_m T)^2 - 2D_0 V_m T \cos q_0 \quad (28)$$

From expression (27) and (28) we can obtain fly-over time  $T$ . When  $V_1$  and flight altitude  $H$  are constant, missile velocity  $V_G$  is constant. Hence,  $V_G t_{f_0} = D_{x_0} = \text{const}$  ( $t_{f_0}$  is preset projectile flight time), i.e., the preset relative launch range  $D_{x_0}$  is a constant. When  $D_0$ ,  $q_0$ ,  $V_1$ , and  $V_m$  are known, we then can obtain  $\tau$  from expressions (17), (19), (21), and (28) and thus we obtain  $f_m$ . With  $V_1 = 600\text{m/s}$  and  $V_m = 500\text{m/s}$ ,  $\tau$  and  $f_m$  obtained for different (initial condition)  $D_0$  and  $q_0$  at several different preset relative launch ranges are listed in Table 2. It is obvious from Table 2 that the maximum frequency component  $f_m$  increases as the occupied approach angle  $q_0$  and preset relative launch range  $D_{x_0}$  decrease. Using the

above computer method for finding a numerical solution for the case where  $D_0 = 7000\text{m}$ ,  $q_0 = 90^\circ$ , and  $D = 300\text{m}$ , we obtained a frequency component of  $0.69\text{Hz}$  which contained 99% of the energy and using the Guillemin impulse approximation method we obtained  $f_m = 0.7\text{Hz}$ . Thus the energy contained within the given bandwidth was over 99%. It is obvious that the approximation method is sufficiently accurate. Its advantage is that the solution of the problem of repetition frequency can simply be summed up as the solution of time constant  $\tau$ , and thus the problem is greatly simplified. It is also suitable for spectrum analysis of various "pass-course" problems.

Table 2. The Minimum Repetition Frequency  $f$  Required for Rangefinding in the Lead-Collision Attack  
( $V_1 = 600\text{m/s}$ ,  $V_m = 500\text{m/s}$ )

$D_{n0}$ (米)(a)	$D_0$ (米)(a)	$q_0$ (度)(b)	$\tau$ (秒)(c)	$f_m = 1/2\tau$ (赫)(d)	$f = 2f_m$ (次/秒)(e)
7,200	10,000	$90^\circ$	7.59	0.065	0.13
7,200	10,000	$150^\circ$	32.60	0.015	0.03
3,600	7,000	$90^\circ$	4.74	0.11	0.22
3,600	7,000	$150^\circ$	16.36	0.03	0.06
300	7,000	$90^\circ$	0.71	0.7	1.4
300	7,000	$150^\circ$	1.14	0.44	0.88

KEY: (a) meters; (b) degrees; (c) seconds; (d) Hz; (e) times/second

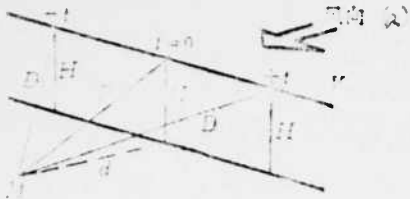
### III. AIR-TO-GROUND AND GROUND-TO-AIR LASER RANGEFINDERS

First we use level bombing as an example to analyze the minimum repetition frequency required when the laser rangefinder is set up as a bomb sight. Based on level bombing principles, in order for the bomb to hit the target the bomb run must be as shown in Figure 4 [2]. Let  $H$  = flight altitude,  $D$  = slant range to target  $M$ ,  $P$  = pass-course slant range,  $V$  = flight speed of the aircraft, and  $d$  = horizontal offset. When  $t = 0$ ,  $D = P$ . Hence, distance  $D$  with change in time  $t$  must satisfy

$$D/P = \{1 + (t/\tau)^2\}^{1/2} \quad (29)$$

where

$$\tau = P/V \quad (30)$$



KEY: (a) wind direction

Fig. 4. Distances in "Pass-Course" Problems with Change in Time

It is obvious that expressions (29) and (30) are identical to expressions (20) and (21). Therefore, expression (26) can be used to find the maximum frequency component  $f_m$ . Table 3 shows the repetition frequencies required after entering the bomb run at a typical flight speed of 300m/s when bombing at low altitude and at medium and high altitude. We can see from Table 3 that the repetition frequency required for low-altitude bombing is much higher than for high-altitude bombing. Therefore, when designing we must take the repetition frequency which satisfies the requirements of low-altitude bombing as the standard.

Table 3. Typical Values for Laser Rangefinder Repetition Frequencies in Bomber Fire Control Systems

	(a) 低空轰炸	(b) 中高空轰炸	(c) 米	(d) 米/秒
$R_{max}$ (c)	120	600	1,200	12,000
$V$ (d)		300		300
$\tau = R/V$ (e)	0.4	2	4	40
$f_m = 1/2\tau$ (f)	1.25	0.25	0.125	0.0125
$f = 2f_m$ (g)	2.5	0.5	0.25	0.025

KEY: (a) low-altitude bombing; (b) medium and high-altitude bombing; (c) meters; (d) meters/second; (e) seconds; (f) Hz; (g) times/second

The repetition frequencies used for ground-to-air laser rangefinders in small anti-aircraft fire control systems are analyzed below. It is common knowledge that small anti-aircraft guns are at the present time effective weapons for low-altitude defense. Since laser rangefinders have good anti-jamming characteristics, superior low-altitude performance, and high ranging accuracy, they have obtained increasingly wide use in small anti-aircraft fire control systems. A typical small anti-aircraft fire control system is

designed under the assumption of the target moving at a constant velocity in a straight line and this approximately holds true during the the brief time of low altitude firing. With the target in level flight, its course is the same as in Figure 4, only point M represents the location of the guns or the rangefinder and d now represents the shortcut [TRANSLATOR'S NOTE: i.e., shortest distance] to the track. With a target velocity of 350m/s, the typical values of required repetition frequencies are shown in Table 4.

Table 4. Typical Values for Laser Rangefinder Repetition Frequencies in Small Anti-aircraft Fire Control Systems  
(V = 350m/s)

H (米)(a)	100		500		1,000	
d (米)(a)	0	100	0	100	0	500
$P = \sqrt{H^2 + d^2}$ (米)(a)	100	141	500	510	1,000	1,118
$\tau = P/V$ (秒)(b)	0.29	0.4	1.43	1.46	2.86	3.19
$f_m = 1/2\tau$ (赫)(c)	1.75	1.25	0.35	0.34	0.175	0.157
$f = 2f_m$ (次/秒)(d)	3.5	2.5	0.7	0.68	0.35	0.31

KEY: (a) meters; (b) seconds; (c) Hz; (d) times/second

It can be seen from Figure 4 that repetition frequency  $f$  increases as flight altitude H and shortcut to track d decrease. Obviously,  $f$  also increases as target velocity increases.

#### IV. BRIEF SUMMARY

This paper has presented a number of methods for determining laser rangefinder repetition frequencies. These methods can be used for correctly selecting repetition frequencies for air-to-air, air-to-ground, and ground-to-air laser rangefinders. Several typical illustrative examples which have been discussed can bring to light some general trends.

1. Repetition frequency  $f$  required for air-to-air rangefinding primarily depends upon the mode of attack. Under conditions where the values of  $V_m$ ,  $V_1$ , and  $\alpha$  are fixed,  $f$  increases as  $q_0$ ,  $D_0$ , or  $D_{x_c}$  decrease. The repetition frequency required in lead-pursuit attack is the highest, and can be more than 8 times/second.



2. The repetition frequency  $f$  required for air-to-ground range-finding primarily depends upon the altitude of the bomber. The  $f$  required for a low-altitude bomber is much greater than that for a high-altitude bomber, with a typical value of more than 2.5 times/second.

3. The repetition frequency  $f$  required for ground-to-air range-finding primarily depends upon target velocity, altitude and track shortcut. For low-altitude, high-speed targets, the  $f$  required for a track shortcut of zero is high, having a typical value of more than 3.5 times/second.

It should be pointed out that in the above discussion it is also assumed that the return rate is 100%. In actuality, the return rate is often less than 100% and the repetition frequency must be increased proportionately. If  $\eta$  is the return rate and  $F$  is the actually required repetition frequency, then under conditions where the system has a reasonable return rate,  $F = f/\eta$ , where  $f$  is the repetition frequency required when  $\eta = 100\%$ . As for the matter of return rates when a laser rangefinder is fitted to various types of tracking systems and fire control systems, this is beyond the scope of the discussion in this paper and will be discussed in another paper.

\* \* \* \*

Computations were carried out on a DJS-14 computer by comrades Xu Li and Zhong Zeyang and the curves in Figures 2 and 3 were made by comrade Duan Wenxin. We hereby express our gratitude to them.

Submitted 26 Jan 1981

#### BIBLIOGRAPHY

- (1) 戴世宗, 数字随动系统, 科学出版社, 1976.
- (2) Airbone Radar, D. Van Norstrand Company, Inc. 1961.
- (3) Burdie, William S., Radar Signal Analysis, Englewood, Califfs. N. J., Prentice-Hall, 1968.
- (4) J. G. Truxal, Automatic Feedback Control System Synthesis, McGraw, 1955.

END

FILMED

4-83

DTIC